Evidence of local structural inhomogeneity in $FeSe_{1-x}Te_x$ from extended x-ray absorption fine structure

B. Joseph,[1] A. Iadecola,[1] A. Puri,[1,2] L. Simonelli,[3]

Y. Mizuguchi,[4] Y. Takano,[4] and N.L. Saini[1,*]

[1]*Dipartimento di Fisica, Università di Roma "La Sapienza",*

P. le Aldo Moro 2, 00185 Roma, Italy

[2]*INFN - Laboratori Nazionali di Frascati,*

Via E. Fermi 40, 00044 Frascati, Rome, Italy

[3]*European Synchrotron Radiation Facility,*

6 RUE Jules Horowitz BP 220 38043 Grenoble Cedex 9 France

[4]*National Institute for Materials Science,*

1-2-1 Sengen, Tsukuba, 305-0047, Japan

JST-TRIP, 1-2-1 Sengen, Tsukuba 305-0047, Japan

Abstract

Local structure of $FeSe_{1-x}Te_x$ has been studied by extended X-ray absorption fine structure (EXAFS) measurements as a function of temperature. Combination of Se and Fe K-edge EXAFS has permitted to quantify the local interatomic distances and their mean-square relative displacements. The Fe-Se and Fe-Te bond lengths in the ternary system are found to be very different from the average crystallographic Fe-Se/Te distance, and almost identical to the Fe-Se and Fe-Te distances for the binary FeSe and FeTe systems, indicating distinct site occupation by the Se and Te atoms. The results provide a clear evidence of local inhomogeneities and coexisting electronic components in the $FeSe_{1-x}Te_x$, characterized by different local structural configurations, with direct implication on the fundamental electronic structure of these superconductors.

PACS numbers: 74.70.Xa;74.81.-g; 61.05.cj

---

*Corresponding author: Naurang.Saini@roma1.infn.it

Among others, an important development in the field of Fe-based superconductors [1] has been the discovery of superconductivity in the FeSe(Te) chalcogenides with the maximum T_c ~15 K [2–4]. Indeed, the PbO-type tetragonal phase of FeSe(Te) has an Fe based planar sublattice, similar to the layered FeAs-based pnictide structures with stacking of edge-sharing Fe(Se,Te)$_4$-tetrahedra layer by layer. Apart from the similar structural topology of active layers, the chalcogenides show structural transition from tetragonal to orthorhombic phase [5–8] analogous to that observed in the FeAs-based pnictides [1, 9]. Also, the interplay between the superconductivity and itinerant magnetism, observed in FeAs-based pnictides [1, 10–12], is well extended to the chalcogenides [13–16]. Therefore, the FeSe(Te) system provides a unique opportunity to study the interplay of the structure, magnetism and superconductivity in the Fe-based families because of the relative chemical simplicity with added advantage of the absence of any spacer layers, that may affect the electronic and structural properties within the active Fe-Fe layers [9].

One of the particularly interesting aspects of chalcogenides is the strong relationship between the superconducting state and the defect chemistry [5, 8]. In addition, the superconducting state can be manipulated by the pressure (either chemical [3, 4, 17] or hydrostatic [14, 18–20]). Over the above, fundamental electronic and magnetic properties are found to show extreme sensitivity to the atomic positions [21, 22] as in the pnictides [22–24]. Therefore, information obtained by diffraction techniques on the average ordered structure of FeSe$_{1-x}$Te$_x$ is not enough to explain the basic electronic properties, and the knowledge of the local structure gets prime importance.

Here, we have used extended X-ray absorption fine structure (EXAFS), a fast and site-specific experimental tool [25] to probe the local structure of FeSe$_{1-x}$Te$_x$ system. For the purpose, we have combined Se and Fe K-edge EXAFS as a function of temperature. The results show that the local environment around the Fe is not homogeneous in the ternary FeSe$_{1-x}$Te$_x$ system, with the Fe-Te and Fe-Se bonds being very different. While the local structure of the FeSe$_{1-x}$ system is consistent with the crystallographic structure, the Se and Te atoms do not occupy the same atomic site in the FeSe$_{1-x}$Te$_x$, breaking the average crystal symmetry.

Temperature dependent X-ray absorption measurements were performed in transmission mode on powder samples of FeSe$_{0.88}$ and FeSe$_{0.5}$Te$_{0.5}$ (Ref. [17]) at the BM29 beamline of the European Synchrotron Radiation Facility (ESRF), Grenoble, using a double crystal

Si(311) monochromator. A continuous flow He cryostat was used to cool the samples with a temperature control within an accuracy of ± 1 K. Standard procedure was used to extract the EXAFS from the absorption spectrum [25].

Figure 1 shows representatives of Fourier transform (FT) magnitudes of the Se K-edge (k-range 3-18Å^{-1}) and Fe K-edge (k-range 3-17Å^{-1}) EXAFS oscillations, measured on FeSe$_{0.88}$ and FeSe$_{0.5}$Te$_{0.5}$ samples, providing partial atomic distribution around the Se and Fe, respectively. The structure of FeSe$_{0.88}$ and FeSe$_{0.5}$Te$_{0.5}$ has tetragonal symmetry at room temperature. For the earlier, a structural transition to an orthorhombic phase appears below ~ 100 K [5, 7, 8]. For the Se site (probed by Se K-edge), there are four Fe near neighbours at a distance ~ 2.4 Å (main peak at ~ 2 Å). The next nearest neighbours of Se are 8 Se(Te) and 4 Fe atoms. Contributions of these distant shells appear mixed, giving a multiple structured peak at ~ 3.0-4.5Å (upper panel). On the other hand, for the Fe site (probed by Fe K-edge) the near neighbours are 4 Se(Te) at a distance ~ 2.4 Å and 4 Fe atoms at a distance ~ 2.6 Å, giving a two peak structure at ~ 1.5-3.0Å (Fig. 1, lower panel), with peaks at longer distances corresponding to longer bond-lengths. Differences in the local structure of two samples can be well appreciated in both Se K and Fe K-edge data with the FTs appearing very different for the two samples.

We will start our discussion on the Se K-edge since first shell EXAFS due to Se-Fe bonds is well separated from the distant shells unlike the Fe K-edge EXAFS in which the contribution of the Fe neighbours (Se/Te and Fe) appear mixed. From the FT itself one can appreciate that the Se-Fe bondlengths in the sample with and without Te are quite similar (see, e.g., upper panel of Fig. 1). The Se-Fe EXAFS has been analyzed using a model with a single distance. On the other hand, following the diffraction results [5–8, 14, 18–20], a three shells model was used for the Fe K-edge EXAFS (due to Fe-Se(Te) bonds and Fe-Fe bonds). The three shells for the FeSe$_{0.88}$ are four Se at ~ 2.4 Å, and 4 Fe (2 each at ~ 2.6 Å and ~ 2.7 Å), and the same for the FeSe$_{0.5}$Te$_{0.5}$ are two Se and two Te atoms at ~ 2.48 Å and four Fe atoms at ~ 2.52 Å. The number of independent data points: N$_{ind} \sim (2\Delta k \Delta R)/\pi$, where Δk and ΔR are respectively the ranges in k and R space over which the data are analyzed [25], were ~ 19 (Δk=15 Å^{-1} and ΔR=2 Å) and ~ 17 (Δk=13 Å^{-1} and ΔR=2 Å) respectively for the Se K-edge (single shell fit) and the Fe K-edge (three shells fit) data. Except the radial distances R$_i$ and related mean square relative displacements (MSRD), determined by the correlated Debye-Waller factor (σ^2), all other parameters were
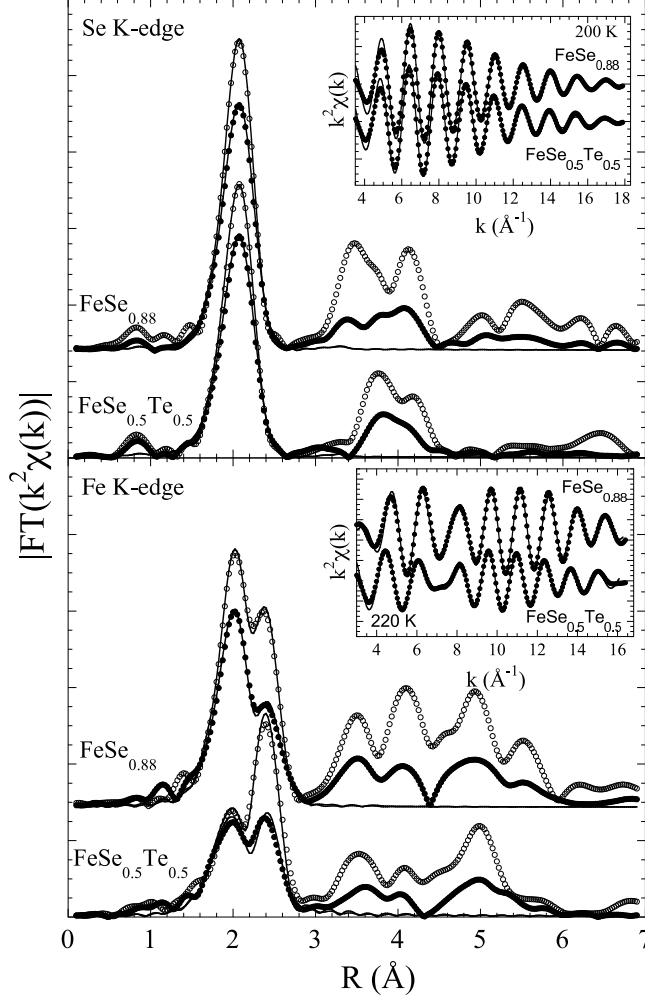
FIG. 1: FT magnitudes of the Se K-edge (upper) and Fe K-edge (lower) EXAFS oscillations at two representative temperatures, measured (symbols) on $FeSe_{0.88}$ (35 K and 200 K) and $FeSe_{0.5}Te_{0.5}$ (35 K and 220 K). The model fits are shown as solid lines. The FTs are not corrected for the phase shifts, and represent raw experimental data. The peaks amplitudes are lower at higher temperature (filled symbols) due to increased MSRD. The insets show representative filtered EXAFS (symbols) with k-space model fits (solid line).

kept constant in the conventional least squares modelling, using the phase and amplitude factors calculated by Feff [26] and exploiting our experience on the studies of similar systems [27]. The representative model model fits to the Se and Fe K-edge EXAFS in the real and k-space are also included in the Fig. 1.

Figure 2 shows temperature dependence of the Fe-Se distances determined from the Se and Fe K-edge EXAFS analysis. The Fe-Se distance in $FeSe_{0.5}Te_{0.5}$ is slightly longer, how-
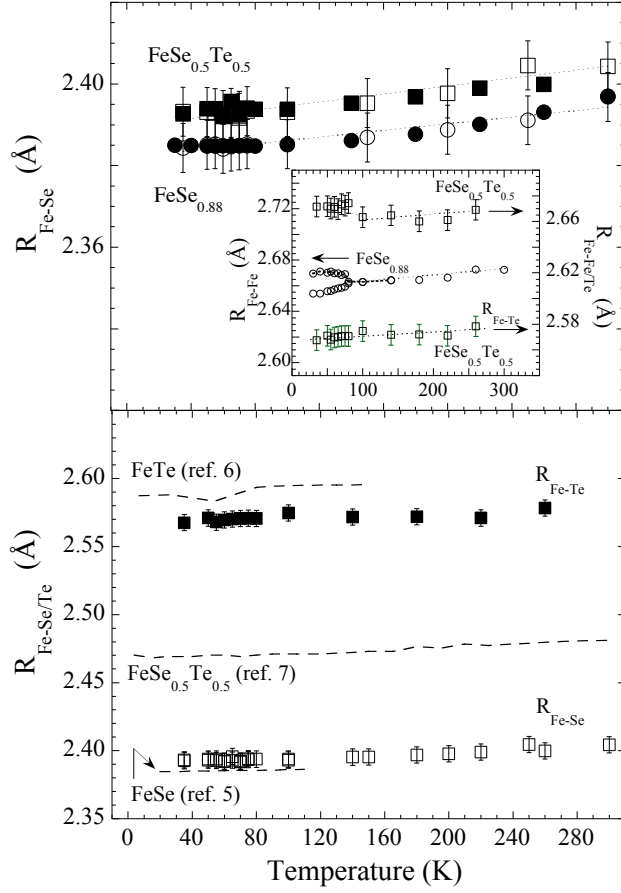
FIG. 2: Temperature dependence of the local Fe-Se bond length (upper panel), determined by Se K-edge (open symbols) and Fe K-edge (filled symbols) for the $FeSe_{0.88}$ (circles) and $FeSe_{0.5}Te_{0.5}$ (squares). The inset shows Fe-Fe and Fe-Te distances for the two samples. The local Fe-Se (open squares) and Fe-Te (filled squares) distances for the $FeSe_{0.5}Te_{0.5}$ are compared with the average diffraction distances (dashed lines) in the lower panel. The average Fe-Te distance in the FeTe system and Fe-Se distance in the FeSe system, are also included. The uncertainties represent average errors, estimated by the standard EXAFS method using correlation maps (Ref. [25]).

ever, the temperature dependence appears similar for the two samples. Other interatomic distances (Fig. 2 inset) are also shown with Fe-Fe distance for the $FeSe_{0.88}$, revealing a small splitting across the structural phase transition at ∼80 K. It was possible to model the data with a single Fe-Fe distance below the structural phase transition, however, inclusion of the two distances, consistent with the diffraction data [5, 19], improved the fit index by about 30%. On the other hand, Fe-Te distance for the $FeSe_{0.5}Te_{0.5}$ appears only slightly shorter than Fe-Te distance for the binary FeTe [6].
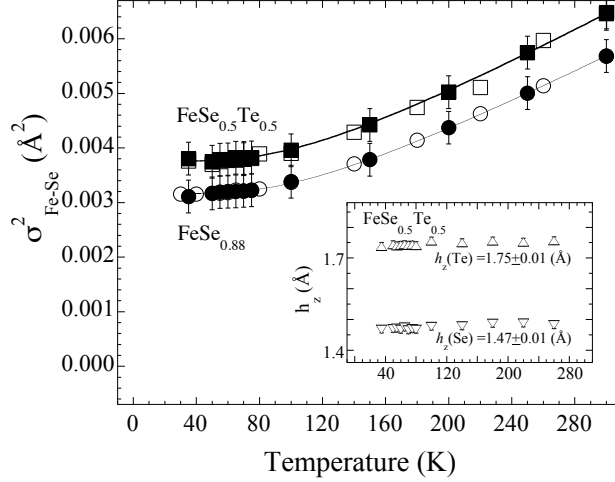
5

FIG. 3: Temperature dependence of the Fe-Se MSRD for the FeSe$_{0.88}$ (circles) and FeSe$_{0.5}$Te$_{0.5}$ (squares), well described by the correlated Einstein model with the Einstein temperature θ_E=300$\pm$20 K (solid lines). The inset shows local Fe-chalcogen heights (h$_z$) in the FeSe$_{0.5}$Te$_{0.5}$ (triangles).

It is interesting to note that, while the local Fe-Se distance for the FeSe$_{0.88}$ is consistent with the average diffraction distance [7, 19], the one for the FeSe$_{0.5}$Te$_{0.5}$ is substantially shorter than the average Fe-Se/Te distance (Fig. 2, lower panel). Indeed, the local Fe-Se distance for the FeSe$_{0.5}$Te$_{0.5}$ is quite similar to the Fe-Se distance in the FeSe$_{0.88}$. Also, the local Fe-Te distance in the FeSe$_{0.5}$Te$_{0.5}$ is only slightly shorter than the average Fe-Te distance for the binary FeTe system [5–7]. The fact that the local Fe-Se (Fe-Te) distance in the FeSe$_{0.5}$Te$_{0.5}$ is almost equal or only slightly longer (shorter) than the Fe-Se (Fe-Te) distance for the FeSe$_{0.88}$ (FeTe) system and much shorter (longer) than the average Fe-Se/Te crystallographic distance, implies that there should be a distribution of the Fe-chalcogen distances at the local scale with Se and Te atoms sitting at different distances from the Fe atoms. This observation not only underlines diverging local structure from the average one for the Te substituted sample, but also constructs a clear evidence for an inhomogeneous distribution of the Fe-Se and Fe-Te bonds and different active electronic components in the chalcogenides.

Figure 3 shows the MSRD (σ^2) of the Fe-Se pair, describing distance-distance correlation function (correlated Debye Waller factors). The EXAFS Debye Waller factors (distance broadening) are different from those measured by diffraction (mean-square displacements,

TABLE I: Comparison between local and average near neighbour distances (and chalcogen heights) in the $FeSe_{0.88}$ and $FeSe_{0.5}Te_{0.5}$.

	Local structure (EXAFS)			Average structure (Diffraction)	
	$R_{Fe-Se}(\text{Å})$	$R_{Fe-Te}(\text{Å})$	$h_z(\text{Å})$	$R_{Fe-Se/Te}(\text{Å})$	$h_z(\text{Å})$
$FeSe_{0.88}$	2.38	-	1.47	2.387	1.46
$FeSe_{0.5}Te_{0.5}$	2.39	2.57	1.47(1.75)	2.471	1.60

i.e. σ_{Fe}^2 and σ_{Se}^2). The MSRD is sum of temperature independent (σ_0^2) and temperature dependent terms, i.e. $\sigma_{Fe-Se}^2 = \sigma_0^2 + \sigma_{Fe-Se}^2$ (T). The MSRD of the Fe-Se pair are well described by the correlated Einstein model [25, 27] with the Einstein temperature $\theta_E = 300\pm20$ K, similar for the two samples within the uncertainties, suggesting similar force constant for the Fe-Se bonds in the two samples. The MSRD for the $FeSe_{0.5}Te_{0.5}$ appears to have slightly higher static component indicating higher disorder, consistent with local structural inhomogeneities [27]. It is worth mentioning that, within the experimental uncertainties, consideration of higher order cumulants in the analysis hardly had any influence on the observed MSRD, consistent with negligible deviation from the Gaussian distributions.

From the measured Fe-Se/Te and Fe-Fe bondlengths, we can determine the local chalcogen height from the Fe-plane (h_z). Since the two chalcogen atoms (Se and Te) occupy two distinct sites in the $FeSe_{0.5}Te_{0.5}$, there are two corresponding h_z, as shown in Fig. 3 (inset). The coexisting Fe-chalcogen heights in the ternary system, showing hardly any temperature dependence, are 1.47 ± 0.01 Å and 1.75 ± 0.01 Å respectively for the Se and Te atoms in the crystallographically homogeneous system. The local near neighbour distances and the Fe-chalcogen heights at a representative temperature (T= 100 K) are shown in table 1 for a quantitative comparison with the diffraction data. Since the Fermi surface topology strongly depends on the chalcogen height [21, 22], the results constructs a direct evidence of local electronic inhomogeneity in the ternary $FeSe_{1-x}Te_x$ system, characterized by distribution of Fe-Se/Te bonds (and hence Fe-chalcogen heights), consistent with the indications of low symmetry structure in the Te substituted FeSe by electron [5] and x-ray diffraction [28].

Let us discuss possible implications of the present study on the fundamental electronic structure of the title system. Low energy electronic states in the Fe-based superconduc-

tors are derived by the five Fe d orbitals with their relative positions modulated by the anion (pnictogen or chalcogen) height [21–24]. The anion height controls the Fermi surface topology (which has strong k_z dispersion), through changing degeneracy between different bands (in particular between the $d_{x^2-y^2}$ and d_{xz}/d_{yz}), with a direct implication on the magnetic structure and superconductivity of the Fe-based materials [29, 30]. For example, it has been clearly shown [21] that a (π,π) like single stripe magnetic order (similar to the Fe-pnictides) is more favorable in the FeSe$_{1-x}$Te$_x$, with small Fe-chalcogen height, unlike a $(\pi,0)$ type double stripe pattern for the FeTe with relatively high Fe-chalcogen height. Therefore, the Fe-chalcogen height seems to control the low energy states, correlation effects (Coloumb screening through hybridizations) and magnetic order, however, this alone is not able to describe the underlying physics. In the light of the above, the observed local inhomogeneity has strong implication on the physics of the chalcogenides, and in general on the Fe-based superconductors. Indeed, the local inhomogeneity, characterized by coexiesting structural configurations with low and high chalcogen heights, can easily reconcile not only the changing magnetic order, but also the photoemission experiments on the FeSe$_{1-x}$Te$_x$ systems [31, 32], debating on surprisingly large effective electron mass and local correlation effects. In addition, the coexisting components can easily modify the Fermi surface topology (and hence the interband scattering and the nesting properties), putting strong constraints on the interpretaion of Fermi surface topological effects and theoretical models describing superconductivity in these materials.

Earlier, we have widely studied the copper oxide perovskites providing clear evidence of inhomogeneous charge distribution characterized by different local structural configurations [27]. The fact that, FeSe$_{1-x}$Te$_x$ system manifest local structural inhomogeneity while the superconducting T$_c$ is higher, provides further indication that the local inhomogeneity should have important role in the new Fe-based materials as well, consistent with recent experiments in favour of mesoscopic phase separation in the Fe-based superconductors [10–13, 15, 33, 34].

In conclusion, we have studied temperature-dependent local structure of the FeSe$_{1-x}$Te$_x$ by combined analysis of Se and Fe K-edge EXAFS. The Fe-Se (Fe-Te) bondlength for the FeSe$_{0.5}$Te$_{0.5}$ is found to be much shorter (longer) than the average Fe-Se/Te, indicating distinct site occupation by the Se and Te atoms and inhomogeneous distribution of the Fe-Se/Te bonds (and hence bond-angles) in a crystallographically homogeneous system. The results provide a clear evidence of local inhomogeneities with coexisting electronic components,

having direct implication on the low lying electronic states and magnetic order, suggesting a possible route to understand the physics of Fe-based chalcogenides.

Acknowledgments

---

[1] K. Ishida, Y. Nakai, and H. Hosono, J. Phys. Soc. Jpn. 78, 062001 (2009).

[2] F.-C. Hsu, et al, Proc. Nat. Acad. Sci. U.S.A. 105, 14262 (2008).

[3] M. H. Fang, H. M. Pham, B. Qian, T. J. Liu, E. K. Vehstedt, Y. Liu, L. Spinu, and Z. Q. Mao, Phys. Rev. B 78, 224503 (2008).

[4] K.-W. Yeh, et al, EPL 84, 37002(2008).

[5] T. M. McQueen, et al, Phys. Rev. B 79, 014522 (2009); T. M. McQueen, A. J. Williams, P. W. Stephens, J. Tao, Y. Zhu, V. Ksenofontov, F. Casper, C. Felser, and R. J. Cava, Phys. Rev. Lett. 103, 057002 (2009).

[6] W.Bao, et al, Phys. Rev. Lett. 102, 247001 (2009).

[7] K. Horigane, H. Hiraka, and K. Ohoyama, J. Phys. Soc. Jpn. 78, 074718 (2009).

[8] E. Pomjakushina, K. Conder, V. Pomjakushin, M. Bendele, and R. Khasanov, Phys. Rev. B 80, 024517 (2009).

[9] M. Fratini, et al, Supercond. Sci. Technol. 21, 092002 (2008).

[10] T. Goko, et al, Phys. Rev. B 80, 024508 (2009).

[11] J. T. Park, et al, Phys. Rev. Lett. 102, 117006 (2009).

[12] K. Kitagawa, N. Katayama, H. Gotou, T. Yagi, K. Ohgushi, T. Matsumoto, Y. Uwatoko, and M. Takigawa, Phys. Rev. Lett. 103, 257002 (2009).

[13] R. Hu, E. S. Bozin, J. B. Warren, and C. Petrovic, Phys. Rev. B 80, 214514 (2009).

[14] S. Medvedev, et al, Nature Mater. 8, 630 (2009).

[15] R. Khasanov, et al, Phys. Rev. B 80, 140511 (2009).

[16] J. Wen, G. Xu, Z. Xu, Z. W. Lin, Q. Li, W. Ratcliff, G. Gu, and J. M. Tranquada, Phys. Rev. B 80, 104506 (2009).

[17] Y. Mizuguchi, F. Tomioka, S. Tsuda, T. Yamaguchi, and Y. Takano, J. Phys. Soc. Jpn. 78, 074712 (2009).

[18] Y. Mizuguchi, F. Tomioka, S. Tsuda, T. Yamaguchi, and Y. Takano, Appl. Phys. Lett. 93, 152505 (2008).

[19] S. Margadonna, Y. Takabayashi, Y. Ohishi, Y. Mizuguchi, Y. Takano, T. Kagayama, T. Nakagawa, M. Takata, and K. Prassides, Phys. Rev. B 80, 064506 (2009); Chem. Commun., 5607-5609 (2008).

[20] K. Horigane, N. Takeshita, C.-H. Lee, H. Hiraka, and K. Yamada, J. Phys. Soc. Jpn. 78, 063705 (2009).

[21] C.-Y. Moon and H. J. Choi, Phys. Rev. Lett. 104, 057003 (2010).

[22] T. Miyake, K. Nakamura, R. Arita, and M. Imada, J. Phys. Soc. Jpn. 79, 044705 (2010).

[23] V. Vildosola, L. Pourovskii, R. Arita, S. Biermann, and A. Georges, Phys. Rev. B 78, 064518 (2008).

[24] M. J. Calderon, B. Valenzuela, and E. Bascones, Phys. Rev. B 80, 094531 (2009).

[25] X-ray Absorption: Principles, Applications, Techniques of EXAFS, SEXAFS, XANES, edited by R. Prins and D. Koningsberger (Wiley, New York, 1988).

[26] J. Mustre de Leon, J. J. Rehr, S. I. Zabinsky, and R. C. Albers, Phys. Rev. B 44, 4146 (1991); J. J. Rehr and R. C. Albers, Rev. Mod. Phys. 72, 621 (2000).

[27] A. Bianconi, N. L. Saini, A. Lanzara, M. Missori, T. Rossetti, H. Oyanagi, H. Yamaguchi, K. Oka, and T. Ito, Phys. Rev. Lett. 76, 3412 (1996); N. L. Saini, A. Lanzara, H. Oyanagi, H. Yamaguchi, K. Oka, T. Ito, and A. Bianconi, Phys. Rev. B 55, 12759 (1997); N. L. Saini, A. Bianconi, and H. Oyanagi, J. Phys. Soc. Jpn. 70, 2092 (2001); N. L. Saini, M. Filippi, H. Oyanagi, H. Ihara, A. Iyo, and A. Bianconi, Phys. Rev. B 68, 104507 (2003); A. Iadecola, S. Agrestini, M. Filippi, L. Simonelli, M. Fratini, B. Joseph, D. Mahajan, and N. L. Saini, EPL 87, 26005 (2009).

[28] M. Tegel, C. Loehnert, and D. Johrendt, Solid State Commun. 150, 383 (2010).

[29] A. Subedi, L. Zhang, D. J. Singh, and M. H. Du, Phys. Rev. B 78, 134514 (2008).

[30] K. Kuroki, H. Usui, S. Onari, R. Arita, and H. Aoki, Phys. Rev. B 79, 224511 (2009).

[31] Y. Xia, D. Qian, L. Wray, D. Hsieh, G. F. Chen, J. L. Luo, N. L. Wang, and M. Z. Hasan, Phys. Rev. Lett. 103, 037002 (2009).

[32] A. Tamai et al, Phys. Rev. Lett. 104, 097002 (2010).

[33] T. Mertelj, V. V. Kabanov, C. Gadermaier, N. D. Zhigadlo, S. Katrych, J. Karpinski, and D. Mihailovic, Phys. Rev. Lett. 102, 117002 (2009).

[34] G. Lang, H. J. Grafe, D. Paar, F. Hammerath, K. Manthey, G. Behr, J. Werner, and B. Buchner, Phys. Rev. Lett. 104, 097001 (2010).